

# Error Detection and Constraint Recovery in Hierarchical Multi-Label Classification without Prior Knowledge

Joshua Shay Kricheli

Arizona State University  
Tempe, Arizona, USA  
jkrichel@asu.edu

Khoa Vo

Arizona State University  
Tempe, Arizona, USA  
ngocbach@asu.edu

Aniruddha Datta

Arizona State University  
Tempe, Arizona, USA  
adatta14@asu.edu

Spencer Ozgur

Arizona State University  
Tempe, Arizona, USA  
sozgur@asu.edu

Paulo Shakarian

Arizona State University  
Tempe, Arizona, USA  
pshak02@asu.edu

## ABSTRACT

Recent advances in Hierarchical Multi-label Classification (HMC), particularly neurosymbolic-based approaches, have demonstrated improved consistency and accuracy by enforcing constraints on a neural model during training. However, such work assumes the existence of such constraints a-priori. In this paper, we relax this strong assumption and present an approach based on Error Detection Rules (EDR) that allow for learning explainable rules about the failure modes of machine learning models. We show that these rules are not only effective in detecting when a machine learning classifier has made an error but also can be leveraged as constraints for HMC, thereby allowing the recovery of explainable constraints even if they are not provided. We show that our approach is effective in detecting machine learning errors and recovering constraints, is noise tolerant, and can function as a source of knowledge for neurosymbolic models on multiple datasets, including a newly introduced military vehicle recognition dataset.

## KEYWORDS

Metacognitive AI, Learning with Constraints, Rule Learning, NeuroSymbolic AI, Hierarchical Multi-label Classification

## 1 INTRODUCTION

Hierarchical Multi-label Classification (HMC) extends the idea of multi-label classification to impose a hierarchy among labels [13, 14, 29, 30] and has been applied to a variety of applications [4, 19, 20]. A separate line of machine learning research deals with the training of a secondary model to identify failures in the first [8, 11, 24, 27] - which has been referred to as “*metacognition*” [17, 21] and typically the secondary model is a black-box model. Recent research trends (specifically neurosymbolic AI [10, 26]) have led to the expression of such hierarchical relationships as constraints on the learning process [4, 13, 33] or leveraging constraints to make corrections to the machine learning model [7, 15]. A key assumption in these approaches is that the constraints are known *a-priori*. Meanwhile, a metacognitive approach known as Error Detection Rules (EDR) allows for the learning of rules to predict failures [32] based on conditions derived from domain knowledge and/or complementary models for the same task trained on the same data. The key intuition of this paper is that we can modify the ideas of [32] to predict

errors and recover constraints of an HMC model without a-prior knowledge of the constraints. Our contributions are as follows:

- We extend the EDR framework of [32] to address the HMC problem without prior knowledge of the hierarchy by both extending the language of that work and presenting a new *Focused-EDR* which addresses an objective function mismatch of [32] by leveraging approximate optimization of the ratio of two submodular functions;
- We demonstrate how our new approach, provides significant improvement in the detection of errors when compared to a black-box baseline neural error detector and the detection algorithm of [32] on three different HMC datasets;
- We show our approach can recover constraints and that both the F1-score of constraints recovered as well as error F1 degrades gracefully with noise - with noise injected in a manner to remove certain classes from consideration;
- We show the recovered constraints can then be used as a source for in neurosymbolic model learning (i.e., Logic Tensor Networks (LTN) [4]) to provide improved model performance and reduce the number of inconsistencies;
- We introduce (and release <sup>1</sup>) an open-source HMC dataset of ~10K images of military vehicles.

The rest of the paper is organized as follows. We provide an overview of related work in Section 2, introduce our Focused EDR approach in Section 3, followed by our experimental results and discussion in Section 4.

## 2 RELATED WORK

In Hierarchical Multi-label Classification (HMC), pre-defined constraints are crucial for shaping effective prediction models [14, 22, 29], which, in general assume that constraints are known a-priori. Neurosymbolic approaches such as [4, 13, 33] also assume the existence of a-prior constraints. In contrast, Semantic Probabilistic Layers (SPL) identify constraint relationships from data but lack explainability, encoding constraints in a deep probabilistic circuit that is not directly interpretable [1]. The approach presented in this work does not assume knowledge of constraints yet allows recovery of interpretable constraints. This work also deals with error detection in ML models or “*metacognition*” [17, 21, 31]. Recent efforts include neurosymbolic methods [7, 9, 16] that rely on

<sup>1</sup><https://github.com/lab-v2/PyEDCR>

**Table 1: Example Error Detection rules for a label  $y$  and violating sets  $V_y$  for several fine and coarse-grain classes ( $\mathcal{Y}_f$  and  $\mathcal{Y}_c$  respectively) of military vehicles. A violating set  $V_y$  is a set of labels which are inconsistent with assigning the class  $y$ .**

Granularity $g$	Label $y$	Error Detecting Rule	Violating Set $V_y$
Coarse-Grain	Tank	$error_{Tank}(X) \leftarrow assign_{Tank}(X) \wedge \bigvee_{y' \in V_y} assign_{y'}(X)$	$\mathcal{Y}_f \setminus \{T-14, T-62, T-64, T-72, T-80, T-90\}$
	SPA	$error_{SPA}(X) \leftarrow assign_{SPA}(X) \wedge \bigvee_{y' \in V_y} assign_{y'}(X)$	$\mathcal{Y}_f \setminus \{2S19-MSTA, BM-30, D-30, Tornado, TOS-1\}$
Fine-Grain	T-14	$error_{T-14}(X) \leftarrow assign_{T-14}(X) \wedge \bigvee_{y' \in V_y} assign_{y'}(X)$	$\mathcal{Y}_c \setminus \{Tank\}$
	2S19-MSTA	$error_{2S19-MSTA}(X) \leftarrow assign_{2S19-MSTA}(X) \wedge \bigvee_{y' \in V_y} assign_{y'}(X)$	$\mathcal{Y}_c \setminus \{SPA\}$

domain knowledge (not an assumption made here). In another line of work, conformal predictions are used to quantify uncertainties and detect errors by generating prediction bands that likely contain the true response [2, 3, 27] - but these black box models do not constructively create constraints as we do here.

**Error Detection Rules (EDR).** EDR was introduced in [32] and is a metacognitive approach for detecting errors in the result of a trained machine learning model  $f_{\hat{\theta}}$  that assigns a label  $y$  for some sample  $x$ . In that work, the logical atom  $assign_y(X)$  means that the model assigned label  $y$  to a sample denoted by the variable symbol  $X$ . Additionally, the method takes a set of boolean conditions  $C$  as input, which are associated with each sample (e.g.,  $cond(X) \equiv True$ , iff condition  $cond$  is true for sample  $x$ ). In practice, these conditions can come from domain knowledge or from a complementary model for the same task (as done in [32]). The key intuition is for each class  $y$  to identify a subset of conditions  $DC_y \subseteq C$  that are indicative of an error made by the model. This results in an *error detection rule*:

$$error_y(X) \leftarrow assign_y(X) \wedge \bigvee_{cond \in DC_y} cond(X). \quad (1)$$

Intuitively, this reads that if one of the conditions in set  $DC_y$  are observed for sample  $X$  and the model assigns class  $y$  to it, then the model has made an error predicting  $x$  to be of class  $y$ . The authors learn the rules through a constrained submodular optimization technique that optimizes target class precision - as opposed to accuracy of detecting errors.

### 3 APPROACH

We now describe some technical preliminaries for our problem and two key extensions we make to the EDR framework of [32]. Specifically, we extend the EDR method to capture the HMC case and we address the objective function mismatch in the detection algorithm. In our setup, we assume that the hierarchical data has  $G$  levels of granularities  $\mathcal{G} := \{g_i\}_{i=1}^G$ , each with a corresponding label set  $\mathcal{Y}_g$ . In this work we focus in the case of  $G = 2$ , and denote  $\mathcal{G} := \{fine, coarse\}$ . The framework can extend for  $G > 2$ , but we leave evaluation of the approach beyond two levels to future work. Let  $\mathcal{X}, \mathcal{Y}$  be all the possible examples and predicted labels, respectively. We thus have  $\mathcal{Y} = \times_{g \in \mathcal{G}} \mathcal{Y}_g$  as all the possible predicted labels, and define  $\mathcal{Y}_{\mathcal{G}} := \bigcup_{g \in \mathcal{G}} \mathcal{Y}_g$ . Define a labeled training set  $\mathcal{T} := \{(x_i^T, gt(x_i^T))\}_{i=1}^{N_{\mathcal{T}}} \subset \mathcal{X} \times \mathcal{Y}$  composed of  $N_{\mathcal{T}}$  images and corresponding ground-truth labels. We assume the existence of a well-trained model  $f_{\hat{\theta}}$  returning one class per level of granularity for a given sample. We then define an *Error Prediction Problem* per class  $y \in \mathcal{Y}_{\mathcal{G}}$ , which is predicting where  $f_{\hat{\theta}}$  predicted  $y$  incorrectly.

We envision such a predictor to be trained on the same data as  $f_{\hat{\theta}}$  and provide a per-example binary output for  $error_y(X)$  (the rule head of (1)), which we refer to as the error class of  $y$ , and denote it  $e_y$ . Earlier work such as [8] relied on a black box model for error predictions, while this paper along with the recent work of [32] utilizes one set of rules per class, as in Expression (1).

**EDR for HMC.** The key difference in employing EDR for HMC problems is that we are detecting errors in  $G > 1$  categories of classes which have hierarchy constraints among them. Hence, we adjust the rules of the form given in Expression (1) for an HMC problem as well as support conditions from multiple models. First, we extend the predicate  $assign$  where we not only have a subscript denoting the class (which can come from multiple granularities) but also a superscript denoting the model, so  $assign_y^f(X)$  means that sample  $x$  was assigned label  $y$  by model  $f$ . Note that the first predicate in the body of the rule (outside the disjunction, as per Expression (1)) will always come from the base model. While [32] primarily relied on domain knowledge for the condition sets, here we use the class predictions from a different label set of the hierarchy. As such, when considering detection rules for any class  $y$ , as in (1), we will consider conditions from the model predictions defined using granularities other than that of  $y$ . Thus for each class  $y$  at granularity  $g$ , we define a specific conditions set  $C_g$  (unlike in [32] where conditions are picked from the same set of conditions as there were no levels of granularity in that paper). The per-granularity condition set will include  $assign$  conditions from the ‘main’ model  $f_{\hat{\theta}}$  across all other granularities, which are  $C_g^{f_{\hat{\theta}}} := \bigcup_{g' \in \mathcal{G} \setminus \{g\}} \bigcup_{y \in \mathcal{Y}_{g'}} \{assign_y^{f_{\hat{\theta}}}\}$ . Since each such  $C_g^{f_{\hat{\theta}}}$  will not include conditions on labels from  $g$ , we also add conditions from a ‘secondary’ model  $h_{\hat{\theta}_h}$ , with a possible different architecture  $h$  and learned parameters  $\hat{\theta}_h$ , for all granularities, i.e.  $C_g^{h_{\hat{\theta}_h}} := \bigcup_{g' \in \mathcal{G}} \bigcup_{y \in \mathcal{Y}_{g'}} \{assign_y^{h_{\hat{\theta}_h}}\}$ . Moreover, similar to what the authors did in [32], we define binary conditions for each label of each granularity which utilize trained binary models  $\{b_{\hat{\theta}_y}\}_{y \in B}$ , given a subset of labels  $B \subseteq \mathcal{Y}_{\mathcal{G}}$ , yielding the binary conditions set  $C_B := \bigcup_{y \in B} \{assign^{b_y}\}$ . Finally, we set the condition set for each granularity to  $C_g := C_g^{f_{\hat{\theta}}} \cup C_g^{h_{\hat{\theta}_h}} \cup C_B$ . We note that in solving the error detection problem for a given label  $y$ , we find a set  $DC_y$  to create a rule of the form seen in Expression (1). Notice how after solving for all the sets  $\{DC_y\}_{y \in \mathcal{Y}_{\mathcal{G}}}$  for an HMC problem, for any granularity  $g$  and label  $y \in \mathcal{Y}_g$ , the conditions in  $DC_y \cap C_g^{f_{\hat{\theta}}}$  are specifying hierarchy constraints, i.e. rules of the form “if label  $y$

is assigned by the model at granularity  $g$  and another label  $y'$  at a different granularity  $g' \neq g$ , then there is an error in assigning  $y$ ." These rules enforce hierarchical consistency, as defined by the ground truth labels. Examples of such rules are given in Table 1.

**Optimization Approach.** As mentioned earlier, in the work of [32], the algorithm that learns the set  $DC_y$  is done so in a way to optimize the precision of  $y$  as opposed to optimizing a metric to detect errors (e.g., as done in [8]). Our key intuition for our optimization approach is that for each label  $y$ , we wish to maximize the F1-score of the error class  $e_y$  (as defined in the *Error Prediction Problem*) as opposed to precision. In this way, we will not only improve error detection, but also recover constraint violations that lead to errors. Our strategy to maximize the error F1 is to identify an equivalent quantity and prove this quantity is the ratio of two submodular functions. This, in turn allows us to leverage the approximation routine of [5] which we later show provides good results in practice. Following the convention of [32] we define  $POS_{DC_y}^T$  as the number of examples in  $\mathcal{T}$  that satisfy any of the conditions in  $DC_y \subseteq C$ , are classified as  $y \in \mathcal{Y}_G$  by  $f_{\hat{\theta}}$  and are also False Positives in the prediction vector of  $f_{\hat{\theta}}$  on  $\mathcal{T}$ , which we will denote  $\hat{Y}_{\hat{\theta}}^T$ . We define  $BOD_{DC_y}^T$  as the number of examples in  $\mathcal{T}$  that satisfy any of the conditions in  $DC_y$  and were predicted as  $y$  in  $\hat{Y}_{\hat{\theta}}^T$ , and  $FP_y^T$  is the number of False Positives of class  $y$  in  $\hat{Y}_{\hat{\theta}}^T$ . For each class  $y$ , we then seek to find an approximate solution to the following optimization problem:

$$DC_y^* \in \operatorname{argmax}_{\emptyset \subset DC_y \subseteq C} \frac{POS_{DC_y}^T}{BOD_{DC_y}^T + FP_y^T}. \quad (2)$$

We note  $POS_{DC_y}^T$  is equivalent to the number of True Positives of  $e_y$  (the error class of  $y$ ) in the training set  $\mathcal{T}$ ,  $BOD_{DC_y}^T$  is the sum of the True and False Positives of  $e_y$  in  $\mathcal{T}$  and  $FP_y^T$  is the sum of the True Positives and False Negatives of  $e_y$  in  $\mathcal{T}$ . Using these, the proof that the quantity in (2) is equal to the F1-score of  $e_y$  in  $\mathcal{T}$  is straightforward. We provide the formal statement below.

**THEOREM 3.1.** *Given a training set  $\mathcal{T}$ , a solution  $DC_y^*$  for the maximization problem in Equation (2) of a class  $y \in \mathcal{Y}_G$  also maximizes the error F1-score for class  $y$  with respect to the prediction vector  $\hat{Y}_{\hat{\theta}}^T$ .*

We note that the quantities of  $POS_{DC_y}^T$  and  $BOD_{DC_y}^T$  are both submodular by Claim 2 of Theorem 4 of [32] while  $FP_y^T$  is a constant for any choice of  $DC_y$ . Hence, the quantity in Expression (2) is the ratio of two submodular functions, which allows us to leverage a variant of Algorithm 3 from [5]. Notice how this algorithm solves for minimizing a ratio of submodular functions  $f/g$ , when the authors of [5] explain in the introduction how the same solution solves the problem of maximizing for  $g/f$ . Thus, we maximize for the ratio in Expression (2) by minimizing for its inverse. The modified algorithm is described in Algorithm 1 in this work. Referring to the runtime described in [5], we note that in the worst case, this algorithm runs in a time complexity of  $O(|C_g|^2)$ , rendering it efficient and scalable as the number of conditions grow.

---

### Algorithm 1 RatioDetRuleLearn

---

**Require:** Class  $y \in \mathcal{Y}_g$  of a granularity  $g$  and its per-granularity condition set  $C_g$

**Ensure:** Non-empty subset of conditions  $\emptyset \subset \hat{DC}_y \subseteq C_g$

$DC_y^0 \leftarrow \emptyset, C_y \leftarrow C_g, i \leftarrow 0$

**while**  $C_y \neq \emptyset$  **do**

$$c_{best} \in \operatorname{argmin}_{c \in C_y} \frac{BOD_{DC_y^i \cup \{c\}}^T - BOD_{DC_y^i}^T}{POS_{DC_y^i \cup \{c\}}^T - POS_{DC_y^i}^T}$$

$$DC_y^{i+1} \leftarrow DC_y^i \cup \{c_{best}\}$$

$$C_y \leftarrow \left\{ c \in C_y \mid POS_{DC_y^{i+1} \cup \{c\}}^T > POS_{DC_y^{i+1}}^T \right\}$$

$i \leftarrow i + 1$

**end while**

$$\hat{i} \in \operatorname{argmin}_i \frac{BOD_{DC_y^i}^T + FP_y^T}{POS_{DC_y^i}^T}$$

**return**  $\hat{DC}_y \leftarrow DC_y^{\hat{i}}$

---

## 4 EXPERIMENTAL RESULTS

We experimented on three datasets in our work - our Military Vehicles dataset and subsets of 50 classes from the ImageNet [25] dataset and 36 classes from the OpenImage [18] dataset. For each of those, we first trained a main model  $f_{\hat{\theta}}$  using the Binary Cross-Entropy (BCE) loss while employing a fitting State of the Art (SOTA) architecture and corresponding hyperparameters which we found to perform favorably among other architecture (the Vision Transformer [12] b\_16 for the Military Vehicles and OpenImage and DINO V2 [23] s\_14 for ImageNet). In the Military Vehicles dataset, there are a total of 9,444 images and we took a ratio of 80 : 20 between train and test. For the ImageNet50 dataset, we kept the original ratio from the paper of 1,300 images in the train set and 50 in the test set for each fine grain class, as well as 2000 train and 400 test images per fine grain class for the OpenImage36 dataset. In all datasets, we had ground truth constraints which we used to compute the fraction of samples violating ground truth constraints in the test set and/or determining the ability to recover constraints.

**Error Detection Results.** For error detection, we evaluated three approaches: Focused EDR (f-EDR, this paper), DetRuleLearn [32], and a neural (black-box) error prediction model inspired by related work (e.g., [8] - with an SOTA neural architecture) that effectively treats error detection as a binary classification problem. For these neural error detection baselines, we used the same model architecture of our base model but retrained for this classification problem. Rules for both f-EDR and DetRuleLearn were trained on the same training data used for the base models. Conditions for the rules were derived from both the class of complementary granularity (e.g., fine for coarse predictions and vice-versa), lesser-performed models trained on the same data, and binary classification models for the same class (much in the same way additional models were used in [32]). We note that both f-EDR and DetRuleLearn used the same set of conditions to learn rules. Results of this experiment are shown in Table 3 where we provide the balanced accuracy and F1-score of the total error - which is defined as applying a logical OR on all the per-class error classes. In all experiments, f-EDR significantly outperforms both DetRuleLearn and the neural-based error

**Table 2: Error Correction Results with LTN**

Dataset	Method	Fine-Grain Acc.	Fine-Grain f1	Coarse-Grain Acc.	Coarse-Grain f1	Inconsistency
Military Vehicles	VIT b_16	54.35%	48.40%	77.24%	74.57%	7.77% (126/1621)
	f-EDR + LTN (ours)	<b>62.43%</b>	<b>58.18%</b>	<b>82.17%</b>	<b>79.95%</b>	<b>5.37%</b> (87/1621)
ImageNet50	DINO V2 s_14	85.76%	85.59%	93.52%	92.65%	1.19% (25/2100)
	f-EDR + LTN (ours)	<b>86.29%</b>	<b>86.12%</b>	<b>93.57%</b>	<b>92.69%</b>	<b>1.05%</b> (22/2100)
OpenImage36	VIT b_16	57.68%	55.89%	90.15%	88.82%	3.02% (362/12002)
	f-EDR + LTN (ours)	<b>60.11%</b>	<b>58.88%</b>	<b>91.21%</b>	<b>89.85%</b>	<b>1.73%</b> (208/12002)

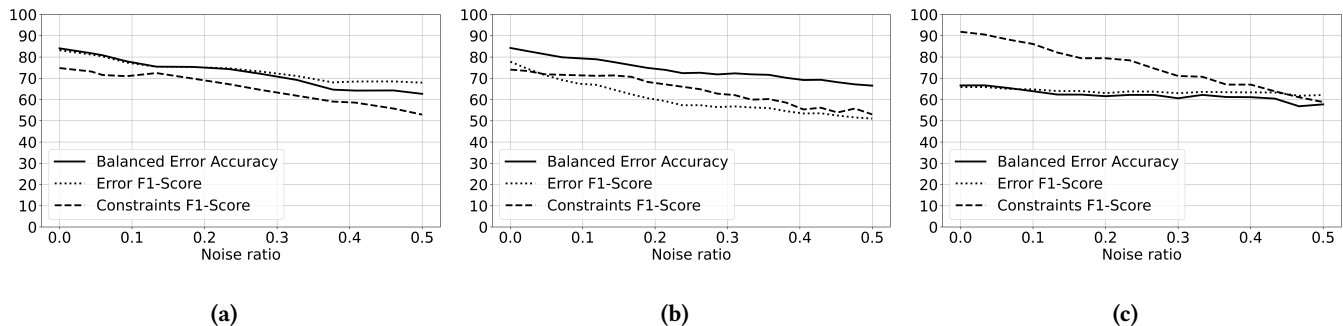


**Figure 1: Balanced Error Accuracy, Error F1-score, and constraints F1-score results of the Focused-EDR method for varying noise ratios for the Military Vehicles (a) ImageNet50 (b) and OpenImage36 (c) datasets**

**Table 3: Error Detection Results for all the datasets**

Dataset	Method	Balanced Error Acc.	Error f1
Military Vehicles	Binary NN	80.10%	80.18%
	DetRuleLearn [32]	83.45%	82.62%
	f-EDR (ours)	<b>84.08%</b>	<b>83.17%</b>
ImageNet50	Binary NN	72.85%	68.96%
	DetRuleLearn [32]	80.92%	72.78%
OpenImage36	f-EDR (ours)	<b>84.26%</b>	<b>77.78%</b>
	Binary NN	64.80%	63.65%
	DetRuleLearn [32]	59.87%	46.46%
	f-EDR (ours)	<b>66.63%</b>	<b>65.83%</b>

prediction by a significant margin in both metrics. These results corroborate the prescribed premise of the method in attempting to maximize for the performance gain of the error class.

**Constraint Recovery and Noise Tolerance.** We also experimented with scenarios involving noisy labels to demonstrate the noise tolerance of our method. In each experiment we pick a subset of fine-grain classes, remove their labels from the ground-truth of the training set and replace them with noisy labels from the remaining fine grain classes. We note that we omit these condition in the models used for conditions (and omit binary models for the removed classes altogether). We experimented with levels of omitted fine grain classes and refer to this as the “noise ratio” (i.e., ratio of fine grain classes omitted to total fine grain classes

available). We then train the whole pipeline from scratch, without any mention of the omitted labels. The results, depicted in Figure 1 include an F1-score on the recovered constraints (compared to a ground truth set of constraints not otherwise used) as well as total error balanced accuracy and F1-score. Three key aspects of these result worth noting are: (1.) we can successfully recover the majority of HMC constraints with our approach, (2.) the recovery of constraints degrades gracefully with incomplete data, (3.) the prediction of errors also degrades gracefully with incomplete data. **Improving Vision Model Performance.** A key envision use-case of this research is to use hierarchical constraints learned with f-EDR to improve the performance of a trained vision model. We compare our baseline model performance with a version whose training is constrained using f-EDR learned rules. Here we utilize rules learned that specify the relationships between fine and coarse grain classes as described in Section 3 and embed constraints in the training process using Logic Tensor Networks (LTN) [4, 6] with an adjusted loss function [28] that considers both error loss and the level of consistency with f-EDR created constraints. Results, shown in Table 2, indicate improved fine grain labels assignment in all cases; improved coarse-grain accuracy and reduced inconsistency (i.e., consistency of assigned classes with ground truth constraints) in all cases. These results show evidence that f-EDR can enhance model performance with a neurosymbolic approach - perhaps avoiding the pressing need for domain knowledge in certain situations.

**Conclusion.** In this paper, we presented a novel approach for detecting failures in HMC models that allows for the recovery of constraints along with error correction, in an explainable and scalable fashion. In future work, we aim to learn more complicated

rules - moving beyond a simple hierarchical relationship, integration of additional knowledge, and applications to control/ autonomy. **Acknowledgement.** This research was Funded by ARO grant W911NF-24-1-0007.

## REFERENCES

- [1] Kareem Ahmed, Stefano Teso, Kai-Wei Chang, Guy Van den Broeck, and Antonio Vergari. 2022. Semantic Probabilistic Layers for Neuro-Symbolic Learning. In *Neural Information Processing Systems*. NIPS 2022, New Orleans, USA, 20. arXiv:2206.00426 [cs.LG]
- [2] Anastasios Angelopoulos, Stephen Bates, Jitendra Malik, and Michael I. Jordan. 2022. Uncertainty Sets for Image Classifiers using Conformal Prediction. arXiv:2009.14193 [cs.CV]
- [3] Anastasios N. Angelopoulos and Stephen Bates. 2022. A Gentle Introduction to Conformal Prediction and Distribution-Free Uncertainty Quantification. arXiv:2107.07511 [cs.LG]
- [4] Samy Badreddine, Artur d'Avila Garcez, Luciano Serafini, and Michael Spranger. 2022. Logic Tensor Networks. *Artificial Intelligence* 303 (2022), 103649.
- [5] Wenruo Bai, Rishabh Iyer, Kai Wei, and Jeff Bilmes. 2016. Algorithms for Optimizing the Ratio of Submodular Functions. In *Proceedings of The 33rd International Conference on Machine Learning (Proceedings of Machine Learning Research, Vol. 48)*, Maria Florina Balcan and Kilian Q. Weinberger (Eds.). PMLR, New York, New York, USA, 2751–2759. <https://proceedings.mlr.press/v48/baib16.html>
- [6] Tommaso Carraro. 2022. *LTNtorch: PyTorch implementation of Logic Tensor Networks*. LTNtorch. <https://doi.org/10.5281/zenodo.6394282>
- [7] Cristina Cornelio, Jan Stuehmer, Shell Xu Hu, and Timothy Hospedales. 2022. Learning where and when to reason in neuro-symbolic inference. In *The Eleventh International Conference on Learning Representations*. ICLR 2022, Kigali, Rwanda, 2 pages.
- [8] Shreyansh Daftry, Sam Zeng, J. Andrew Bagnell, and Martial Hebert. 2016. Inrospective Perception: Learning to Predict Failures in Vision Systems. <https://doi.org/10.48550/arXiv.1607.08665> arXiv:1607.08665 [cs]
- [9] Wang-Zhou Dai, Qiuling Xu, Yang Yu, and Zhi-Hua Zhou. 2019. Bridging machine learning and logical reasoning by abductive learning. *Advances in Neural Information Processing Systems* 32 (2019), 12 pages.
- [10] Artur d'Avila Garcez and Luis C. Lamb. 2020. Neurosymbolic AI: The 3rd Wave. *CoRR* abs/2012.05876 (2020).
- [11] Harrison Delecki, Masha Itkina, Bernard Lange, Ransalu Senanayake, and Mykel J. Kochenderfer. 2022. How Do We Fail? Stress Testing Perception in Autonomous Vehicles. In *2022 IEEE/RSJ International Conference on Intelligent Robots and Systems (IROS)*, 5139–5146. <https://doi.org/10.1109/IROS47612.2022.9981724>
- [12] Alexey Dosovitskiy, Lucas Beyer, Alexander Kolesnikov, Dirk Weissenborn, Xi-aohua Zhai, Thomas Unterthiner, Mostafa Dehghani, Matthias Minderer, Georg Heigold, Sylvain Gelly, Jakob Uszkoreit, and Neil Houlsby. 2021. An Iaesage is Worth 16x16 Words: Transformers for Image Recognition at Scale. In *International Conference on Learning Representations*. ICLR, Vienna, Austria, 21 pages. <https://openreview.net/forum?id=YicbFdNTTy>
- [13] Eleonora Giunchiglia and Thomas Lukasiewicz. 2020. Coherent hierarchical multi-label classification networks. In *Proceedings of the 34th International Conference on Neural Information Processing Systems (Vancouver, BC, Canada) (NIPS'20)*. Curran Associates Inc., Red Hook, NY, USA, Article 810, 12 pages.
- [14] Wei Huang, Enhong Chen, Qi Liu, Hui Xiong, Zhenya Huang, Shiwei Tong, and Dan Zhang. 2023. HmcNet: A General Approach for Hierarchical Multi-Label Classification. *IEEE Transactions on Knowledge and Data Engineering* 35, 9 (2023), 8713–8728. <https://doi.org/10.1109/TKDE.2022.3207511>
- [15] Yu-Xuan Huang, Wang-Zhou Dai, Yuan Jiang, and Zhi-Hua Zhou. 2023. Enabling Knowledge Refinement upon New Concepts in Abductive Learning. *Proceedings of the AAAI Conference on Artificial Intelligence* 37, 7 (Jun. 2023), 7928–7935. <https://doi.org/10.1609/aaai.v37i7.25959>
- [16] Yu-Xuan Huang, Wang-Zhou Dai, Yuan Jiang, and Zhi-Hua Zhou. 2023. Enabling Knowledge Refinement upon New Concepts in Abductive Learning. *Proceedings of the AAAI Conference on Artificial Intelligence* 37 (2023), 8 pages.
- [17] Bonnie Johnson. 2022. Metacognition for artificial intelligence system safety – An approach to safe and desired behavior. *Safety Science* 151 (2022), 105743. <https://doi.org/10.1016/j.ssci.2022.105743>
- [18] Alina Kuznetsova, Hassan Rom, Neil Alldrin, Jasper Uijlings, Ivan Krasin, Jordi Pont-Tuset, Shahab Kamali, Stefan Popov, Matteo Mallocci, Alexander Kolesnikov, Tom Duerig, and Vittorio Ferrari. 2020. The Open Images Dataset V4: Unified Image Classification, Object Detection, and Visual Relationship Detection at Scale. *International Journal of Computer Vision* 128, 7 (March 2020), 1956–1981. <https://doi.org/10.1007/s11263-020-01316-z>
- [19] Rundong Liu, Wenhan Liang, Weijun Luo, Yuxiang Song, He Zhang, Ruohua Xu, Yunfeng Li, and Ming Liu. 2023. Recent Advances in Hierarchical Multi-label Text Classification: A Survey. arXiv:2307.16265 [cs.CL]
- [20] Zhongchen Ma, Zongpeng Li, and Yongzhao Zhan. 2022. Deep Large-Margin Rank Loss for Multi-Label Image Classification. *Mathematics* 10, 23 (2022), 14 pages. <https://doi.org/10.3390/math10234584>
- [21] Pattie Maes and Daniele Nardi. 1988. Meta-Level Architectures and Reflection. In *Meta-level architectures and reflection*. Elsevier Science Pub. Co., Amsterdam, Netherlands, 355. <https://api.semanticscholar.org/CorpusID:60607042>
- [22] Khondaker Tasrif Noor, Antonio Robles-Kelly, and Brano Kusy. 2022. A Capsule Network for Hierarchical Multi-Label Image Classification. arXiv:2209.05723 [cs.CV]
- [23] Maxime Oquab, Timothée Darcet, Théo Moutakanni, Huy Vo, Marc Szafraniec, Vasil Khalidov, Pierre Fernandez, Daniel Haziza, Francisco Massa, Alaaeldin El-Nouby, Mahmoud Assran, Nicolas Ballas, Wojciech Galuba, Russell Howes, Po-Yao Huang, Shang-Wen Li, Ishan Misra, Michael Rabbat, Vasu Sharma, Gabriel Synnaeve, Hu Xu, Hervé Jegou, Julien Mairal, Patrick Labatut, Armand Joulin, and Piotr Bojanowski. 2024. DINOv2: Learning Robust Visual Features without Supervision. arXiv:2304.07193 [cs.CV]
- [24] Manikandasriram Srinivasan Ramanagopal, Cyrus Anderson, Ram Vasudevan, and Matthew Johnson-Roberson. 2018. Failing to Learn: Autonomously Identifying Perception Failures for Self-driving Cars. 3, 4 (2018), 3860–3867. <https://doi.org/10.1109/LRA.2018.2857402> arXiv:1707.00051 [cs]
- [25] Olga Russakovsky, Jia Deng, Hao Su, Jonathan Krause, Sanjeev Satheesh, Sean Ma, Zhiheng Huang, Andrej Karpathy, Aditya Khosla, Michael Bernstein, Alexander C. Berg, and Li Fei-Fei. 2015. ImageNet Large Scale Visual Recognition Challenge. arXiv:1409.0575 [cs.CV]
- [26] Paulo Shakarian, Chitta Baral, Gerardo I. Simari, Bowen Xi, and Lahari Pokala. 2023. *Neuro Symbolic Reasoning and Learning*. Springer, United States. <https://doi.org/10.1007/978-3-031-39179-8>
- [27] Jiankai Sun, Yiqi Jiang, Jianing Qiu, Parth Nobel, Mykel J Kochenderfer, and Mac Schwager. 2023. Conformal Prediction for Uncertainty-Aware Planning with Diffusion Dynamics Model. In *Advances in Neural Information Processing Systems*, A. Oh, T. Naumann, A. Globerson, K. Saenko, M. Hardt, and S. Levine (Eds.), Vol. 36. Curran Associates, Inc., 80324–80337. [https://proceedings.neurips.cc/paper\\_files/paper/2023/file/fe318a2b6c699808019a456b706cd845-Paper-Conference.pdf](https://proceedings.neurips.cc/paper_files/paper/2023/file/fe318a2b6c699808019a456b706cd845-Paper-Conference.pdf)
- [28] Simon Vandenhende, Stamatios Georgoulis, Wouter Van Gansbeke, Marc Proesmans, Dengxin Dai, and Luc Van Gool. 2021. Multi-Task Learning for Dense Prediction Tasks: A Survey. *IEEE Transactions on Pattern Analysis and Machine Intelligence* (2021), 1–1. <https://doi.org/10.1109/tpami.2021.3054719>
- [29] Celine Vens, Jan Struyf, Leander Schietgat, Sašo Džeroski, and Hendrik Blockeel. 2008. Decision trees for hierarchical multi-label classification. *Machine Learning* 73 (11 2008), 185–214. <https://doi.org/10.1007/s10994-008-5077-3>
- [30] Jonatas Wehrmann, Ricardo Cerri, and Rodrigo Barros. 2018. Hierarchical Multi-Label Classification Networks. In *Proceedings of the 35th International Conference on Machine Learning (Proceedings of Machine Learning Research, Vol. 80)*, Jennifer Dy and Andreas Krause (Eds.). PMLR, New York, USA, 5075–5084. <https://proceedings.mlr.press/v80/wehrmann18a.html>
- [31] Benjamin D. Werner, Benjamin J. Schumeg, Jason E. Summers, and Visar Berisha. 2024. Machine Learning Qualification Process and Impact to System Assurance. In *2024 Annual Reliability and Maintainability Symposium (RAMS)*, 1–6. <https://doi.org/10.1109/RAMS51492.2024.10457743>
- [32] Bowen Xi, Kevin Scaria, and Paulo Shakarian. 2023. Rule-Based Error Detection and Correction to Operationalize Movement Trajectory Classification. arXiv:2308.14250 [cs.LG]
- [33] Jingyi Xu, Zilu Zhang, Tal Friedman, Yitao Liang, and Guy Van den Broeck. 2018. A Semantic Loss Function for Deep Learning with Symbolic Knowledge. arXiv:1711.11157 [cs.AI]